Supporting Information

Stretchable Solid-State Zinc Ion Battery Based on Cellulose Nanofiber-Polyacrylamide Hydrogel Electrolyte and $Mg_{0.23}V_2O_5 \cdot 1.0H_2O$ Cathode

Wangwang Xu[a], Chaozheng Liu[b], Qinglin Wu[a,] *, Weiwei Xie[c], Won-Young Kim[d], Sang-Young Lee[d] , and Jaegyoung Gwon[e]

[a] School of Renewable Natural Resources, Louisiana State University AgCenter, Baton Rouge, Louisiana 70803, United States

[b] College of Materials Science and Engineering, Nanjing Forestry University, Nanjing, China

[c] Department of Chemistry, Louisiana State University, Baton Rouge, Louisiana 70803, United States

[d] Department of Energy Engineering, School of Energy and Chemical Engineering, Ulsan National Institute of Science and Technology (UNIST), Ulsan 689-798, South Korea.

[e] Forest Products Department, National Institute of Forest Science, 57 Hoegiro, Dongdaemun-gu, Seoul 02455, South Korea.

* Corresponding Author.

E-mail: qwu@agcenter.lsu.edu (Q. Wu). Phone: 225-578-8369. Fax: 225-578-4251.

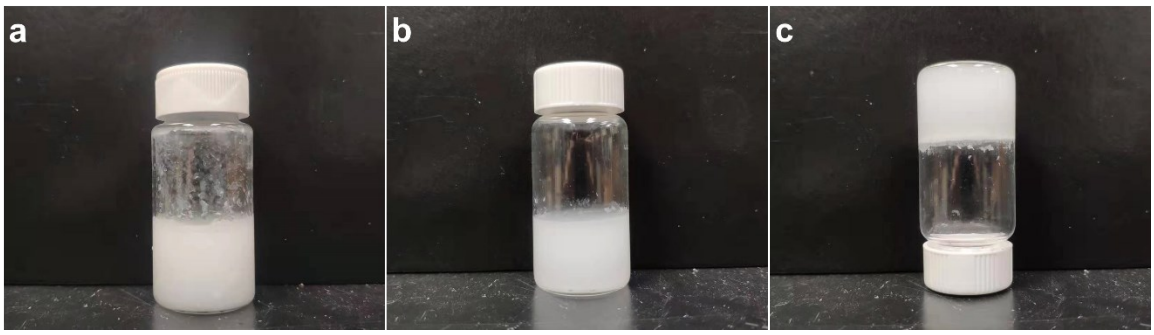

Figure S1. Photos of CNF and CNF-PAM solid-state electrolytes. (a) CNF dispersed in the solution of 1 M $Zn(CF_3SO_3)_2$; (b), (c) CNF-PAM prepared by the radical polymerization.

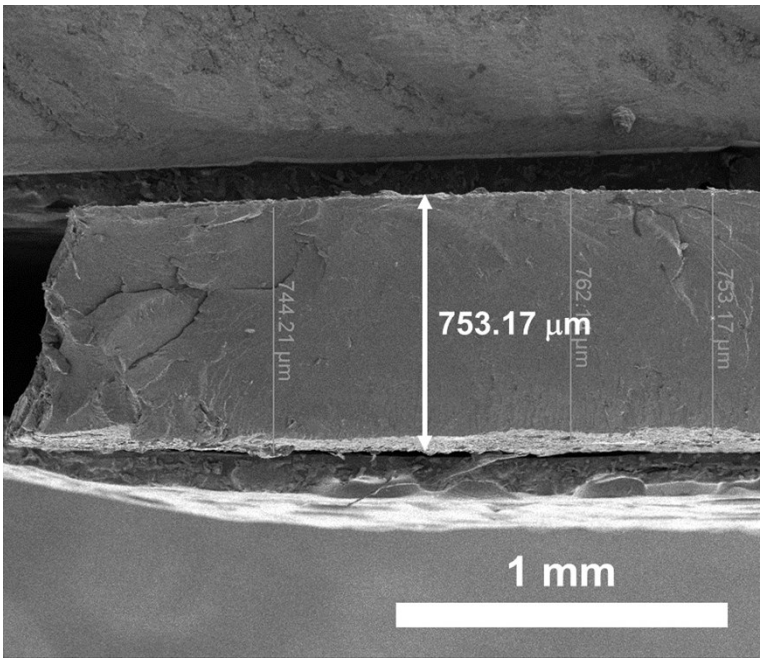

Figure S2. Cross-section SEM image of CNF-PAM film.

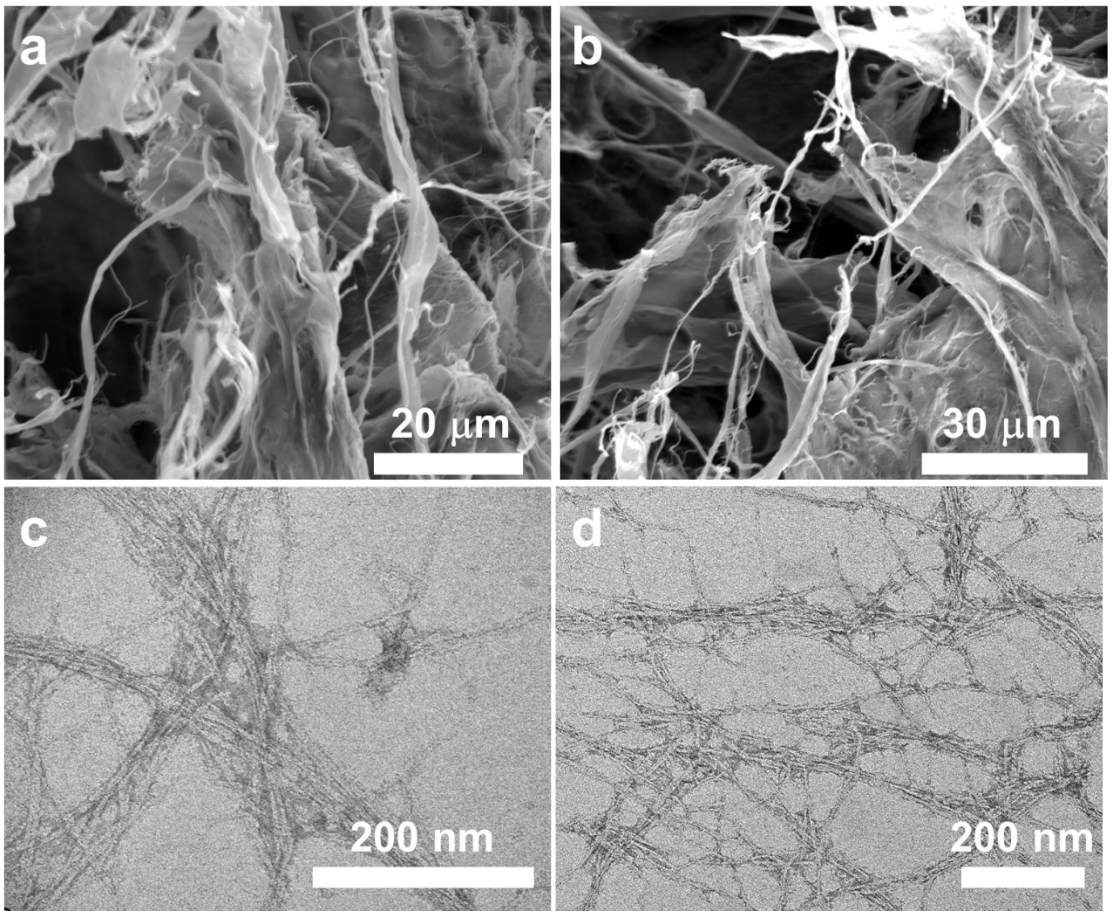

Figure S3. SEM (a, b) and TEM (c, d) images of CNFs

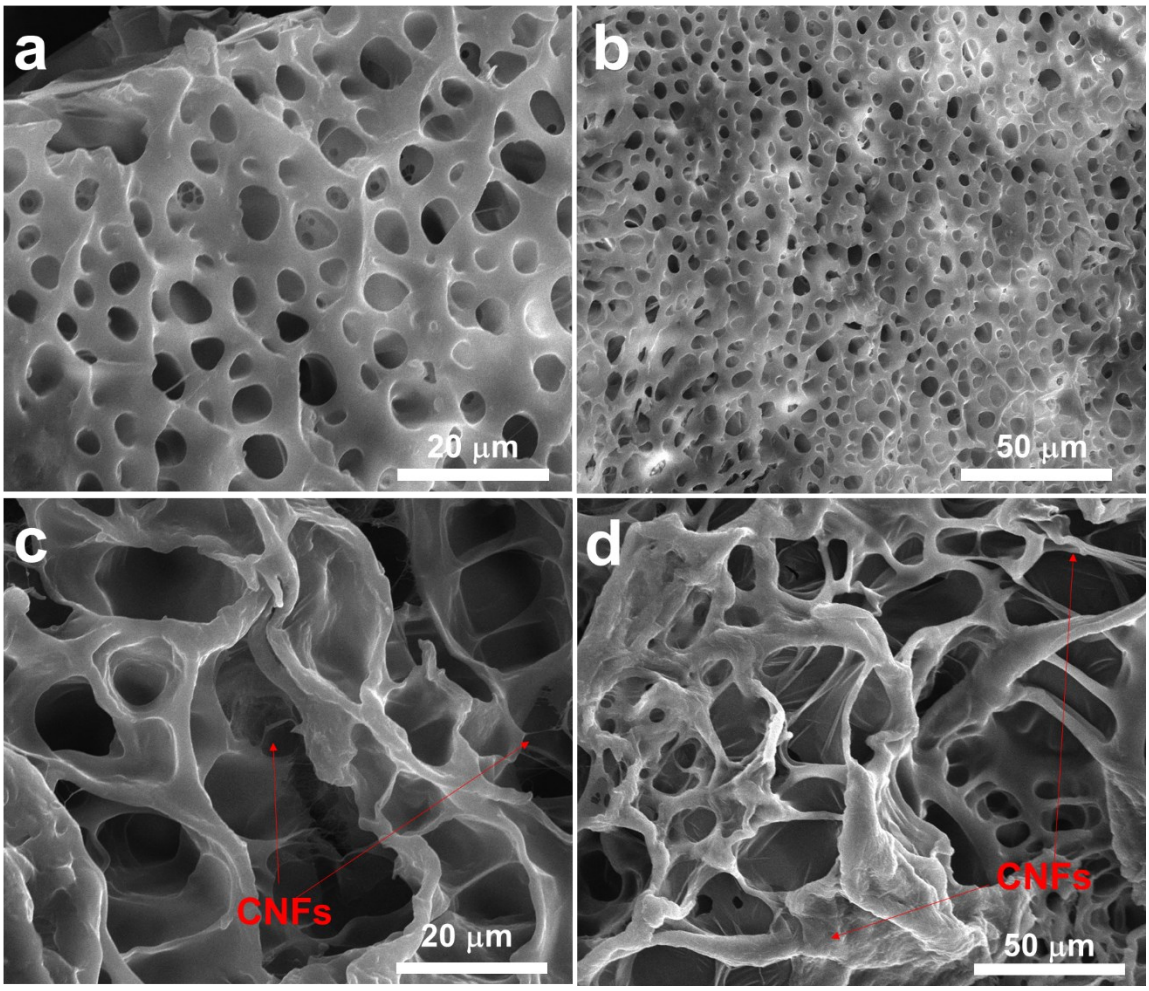

Figure S4. SEM images of (a, b) freeze-dried PAM film and (c, d) freeze-dried CNF-PAM films

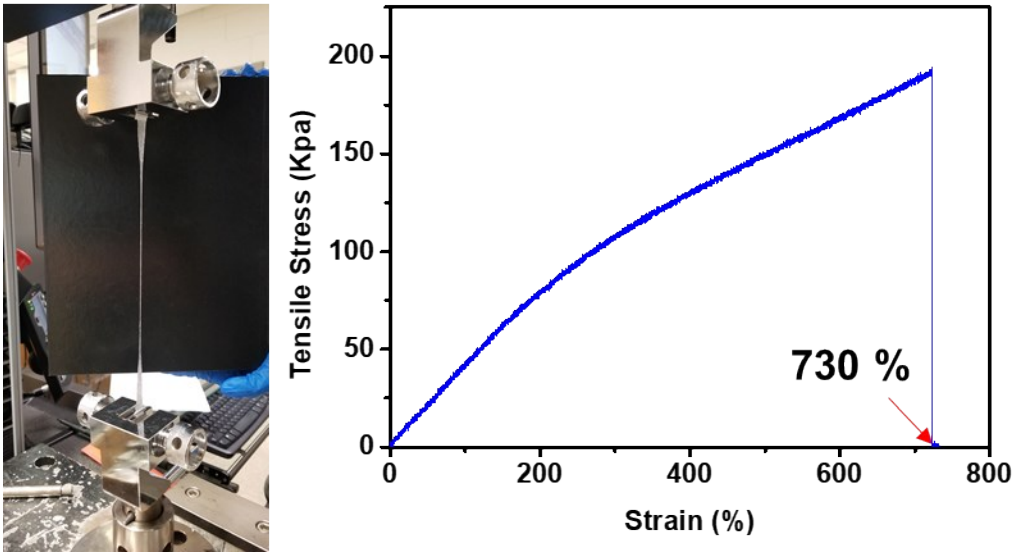

Figure S5. Stress–strain curves of CFC/PAM hydrogel film

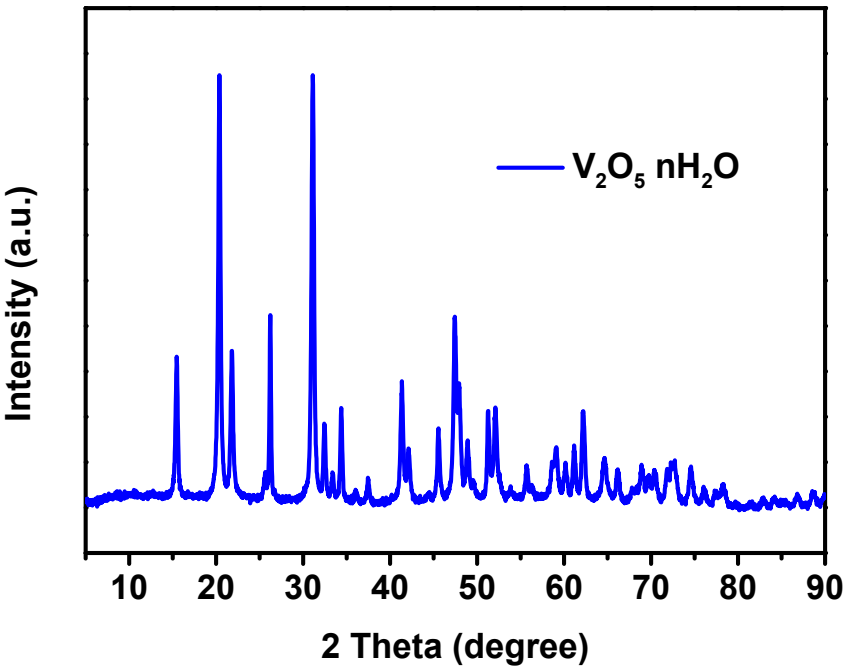

Figure S6. XRD pattern of $V_2O_5 \cdot nH_2O$.

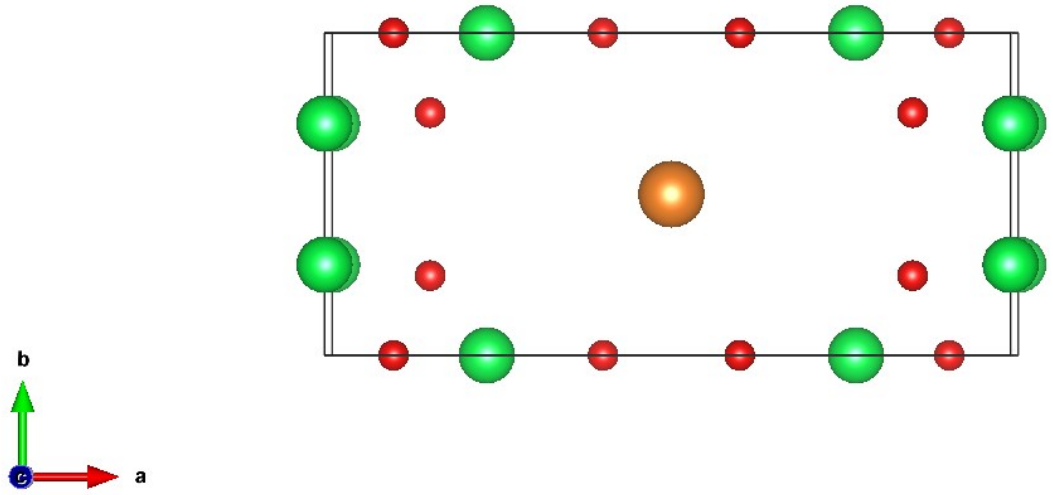

Figure S7. Crystal structure of $Mg_{0.23}V_2O_5 \cdot 1.0H_2O$ microspheres viewed from c axis.

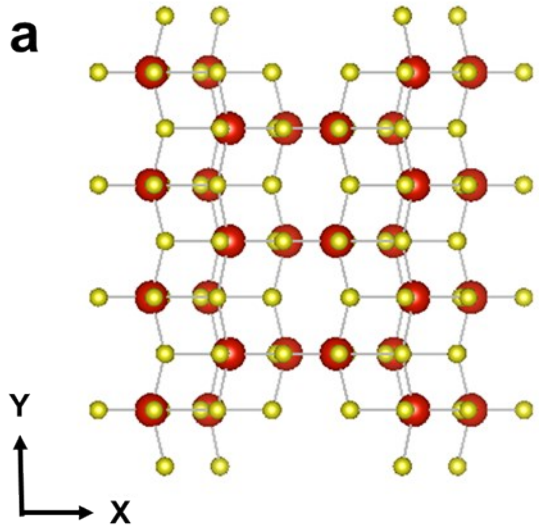

Figure S8. Crystal structure of $Mg_{0.23}V_2O_5 \cdot 1.0H_2O$ microspheres in (a) xy, and (b) vanadium environments. The V atoms are shown by red ball, and O atoms are shown by yellow balls.

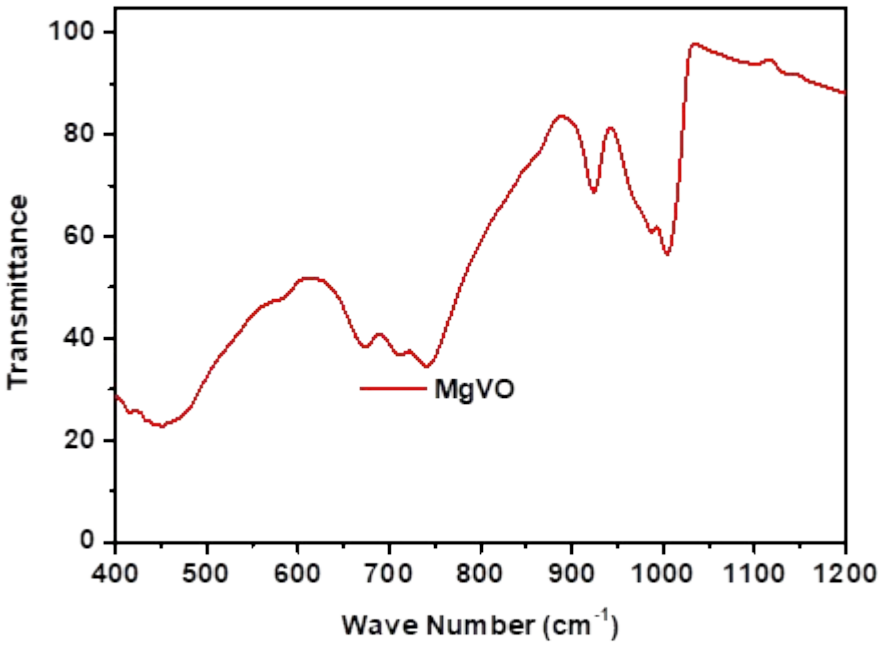

Figure S9. FTIR spectrum of $Mg_{0.23}V_2O_5 \cdot 1.0H_2O$ microspheres.

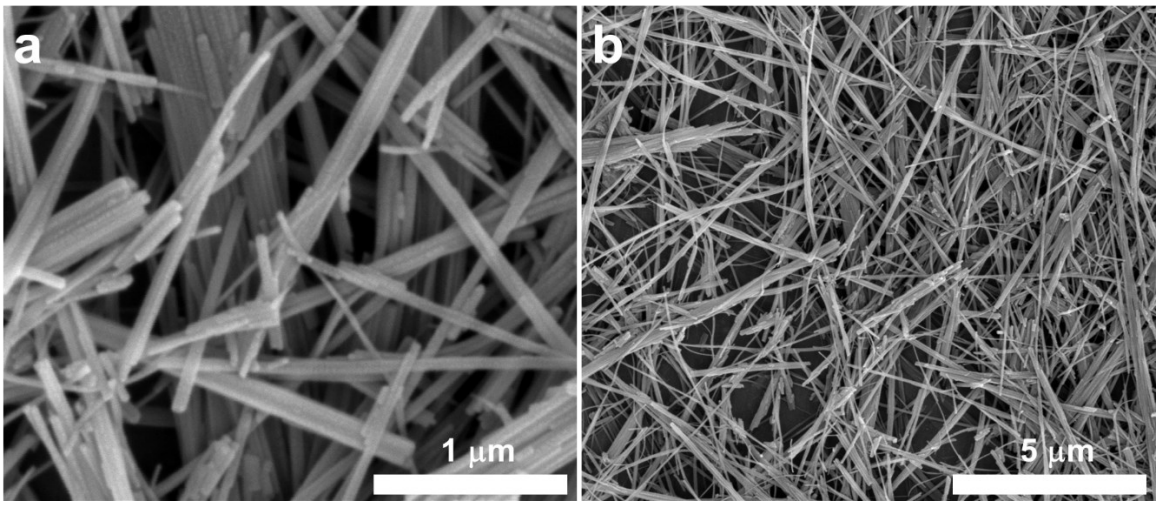

Figure S10. SEM images of $V_2O_5 \cdot nH_2O$ nanowires.

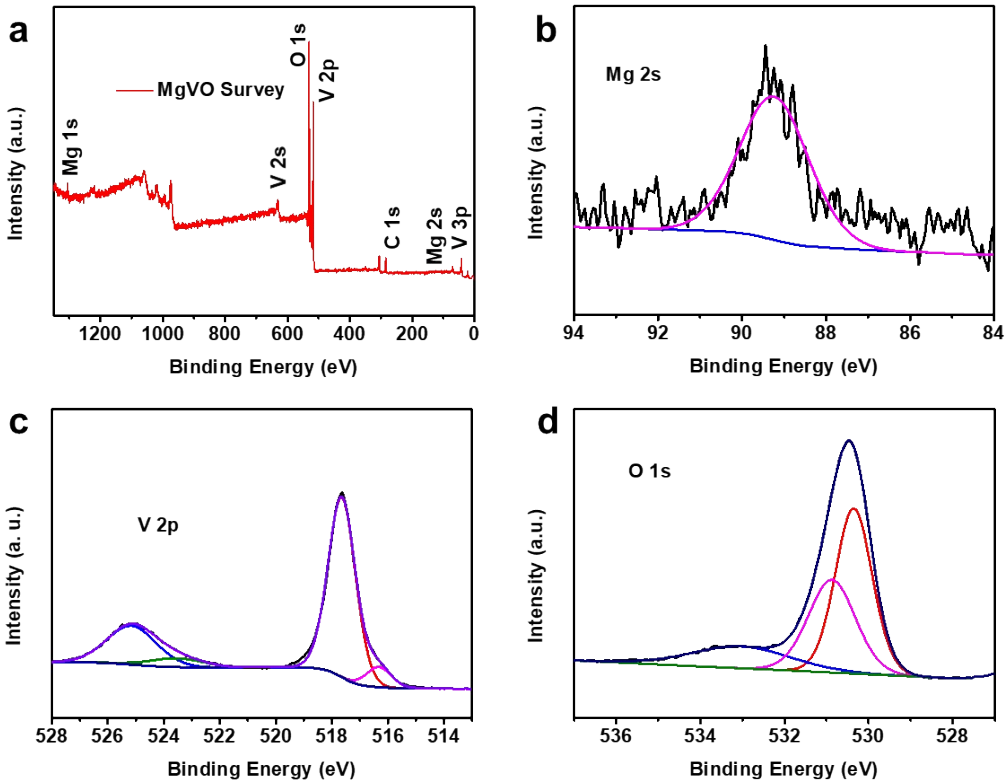

Figure S11. XPS spectrum of $Mg_{0.23}V_2O_5{\cdot}1.0H_2O$ microspheres. (a) XPS survey, high-resolution XPS spectrum of (b) Mg 2s, (c) V2p, (d) O 1s.

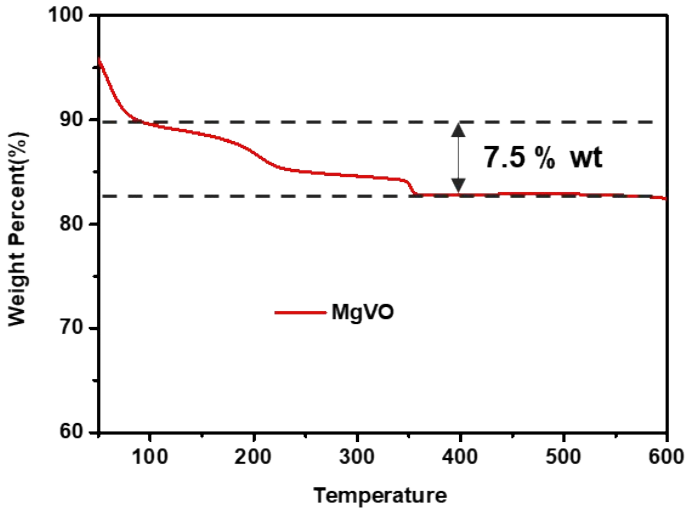

Figure S12. TGA curve of the prepared $Mg_{0.23}V_2O_5 \cdot 1.0H_2O$ microspheres.

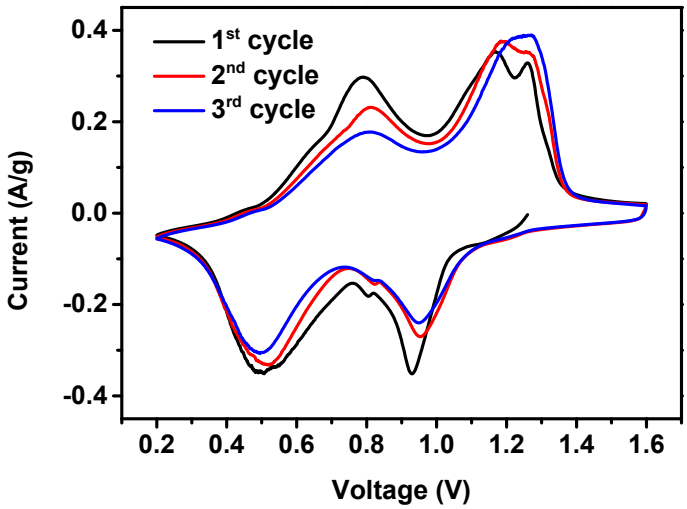

Figure S13. CV curves of MVO/Zn solid-state batteries during the first three cycles at 0.1 mV/s.

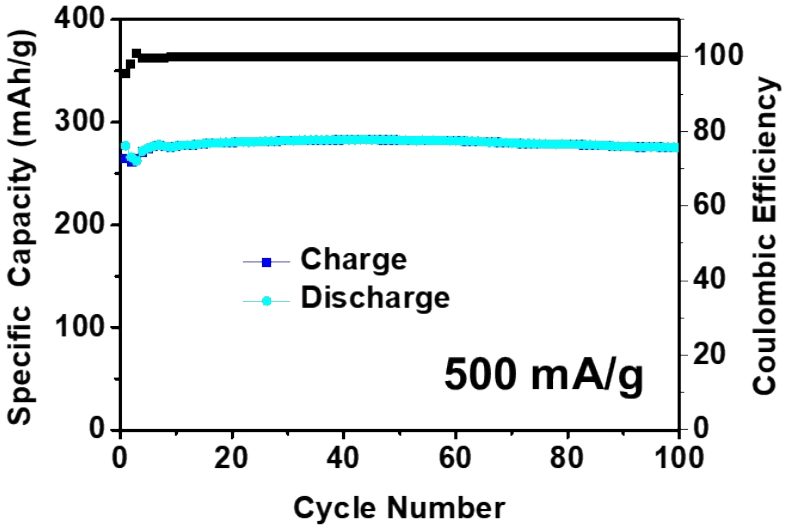

Figure S14. Cycling performance of $V_2O_5 \cdot nH_2O$ at current density of 500 mA/g.

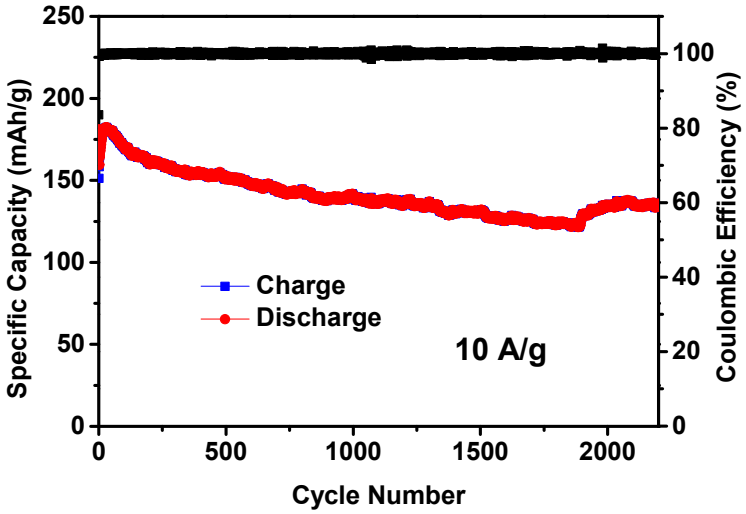

Figure S15. Cycling performance at current density of10 A/g.

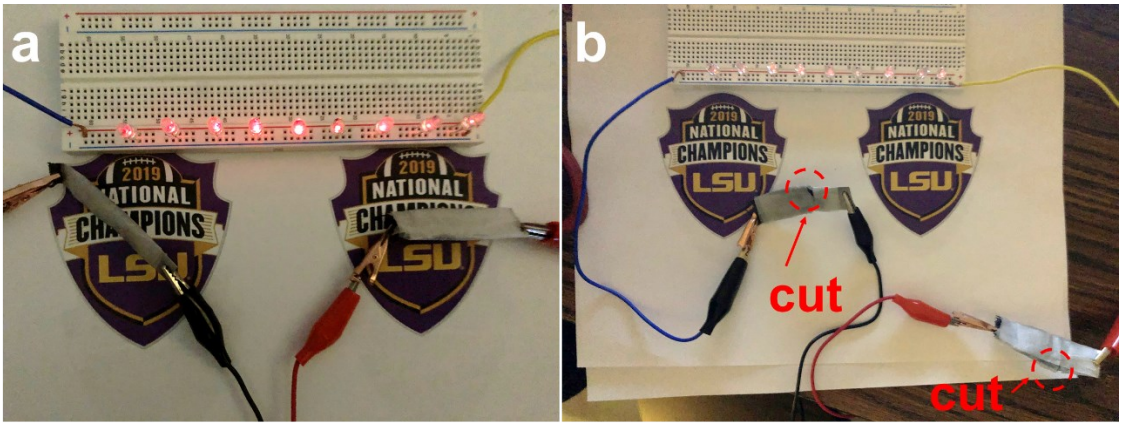

Figure S16. Optical photos of (a, b) CNF and (c, d) CNF-PAM films

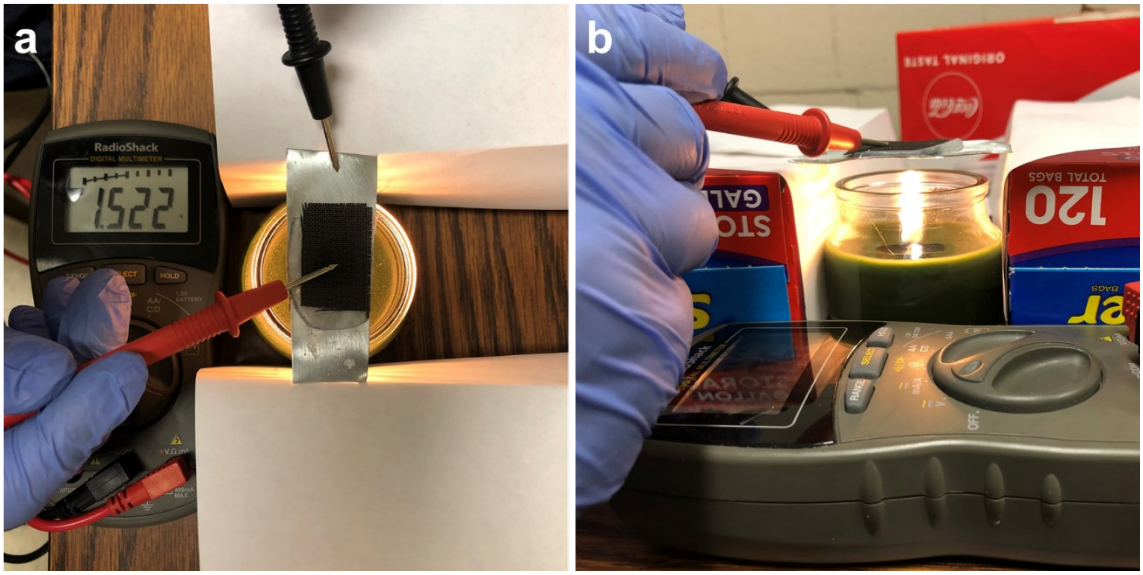

Figure S17. Optical photos of MVO/Zn solid-state ZIB with burning.

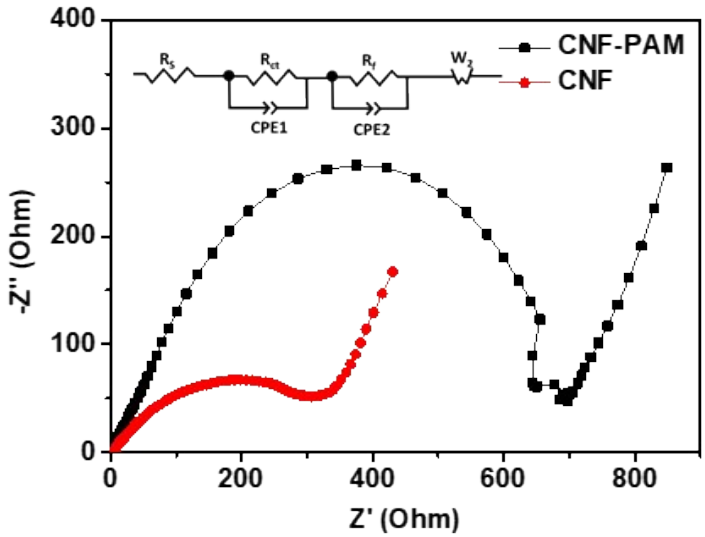

Figure S18. Nyquist plots of solid-state MVO/Zn batteries using CNF-PAM film and CNF film as electrolyte.

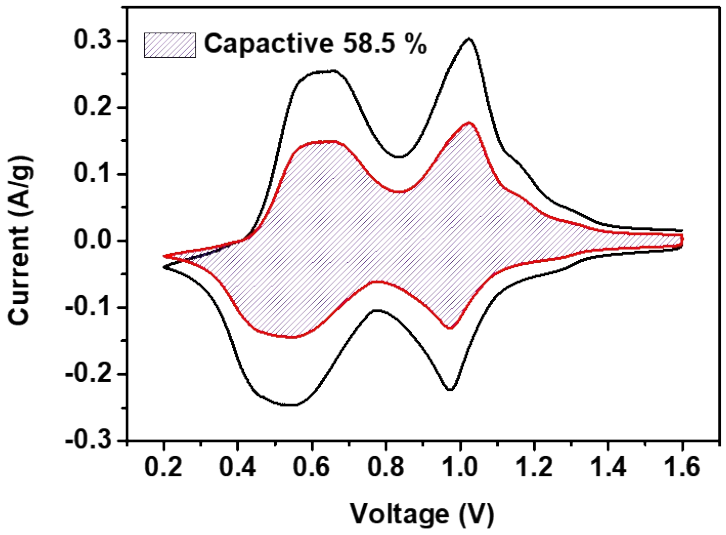

Figure S19. The CV curve at 0.1 mV/s. (The shaded area shows the capacitive contributions)

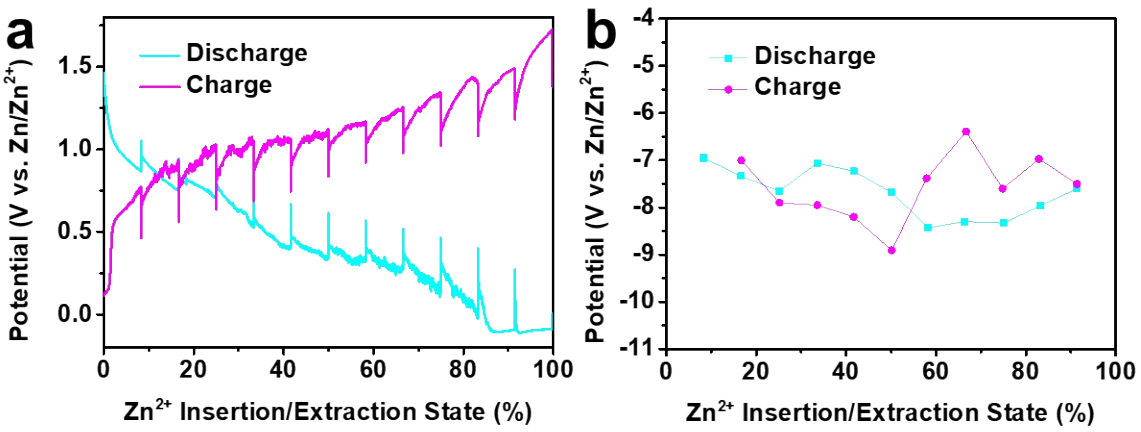

Figure S20. GITT profiles of $V_2O_5 \cdot 1.0H_2O$ based solid-state ZIBs, (e) diffusion versus different Zn^{2+} insertion/extraction states,

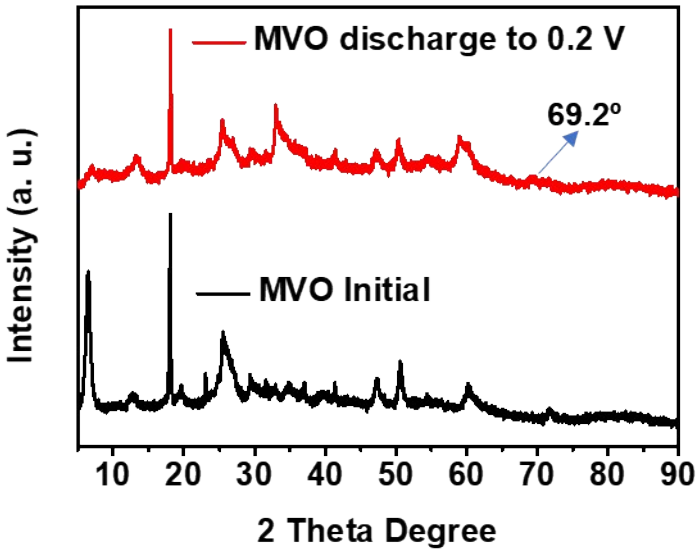

Figure S21. XRD of MVO at initial and fully discharge states.

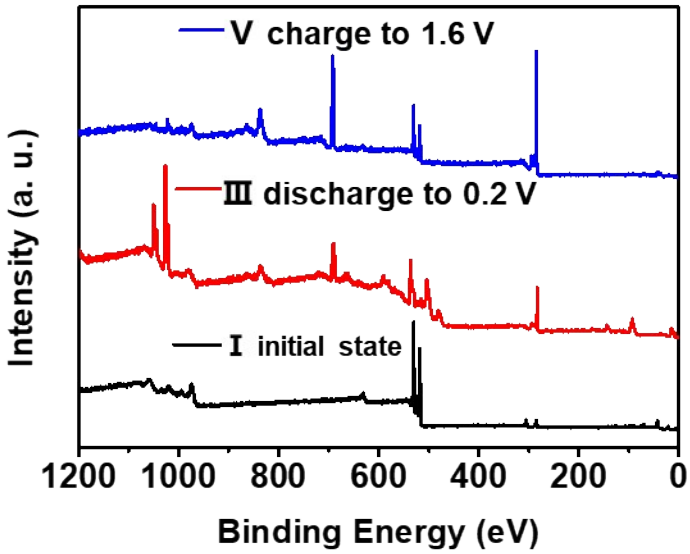

Figure S22. XPS survey of $Mg_{0.23}V_2O_5 \cdot 1.0H_2O$ microspheres at different charging/discharging states.

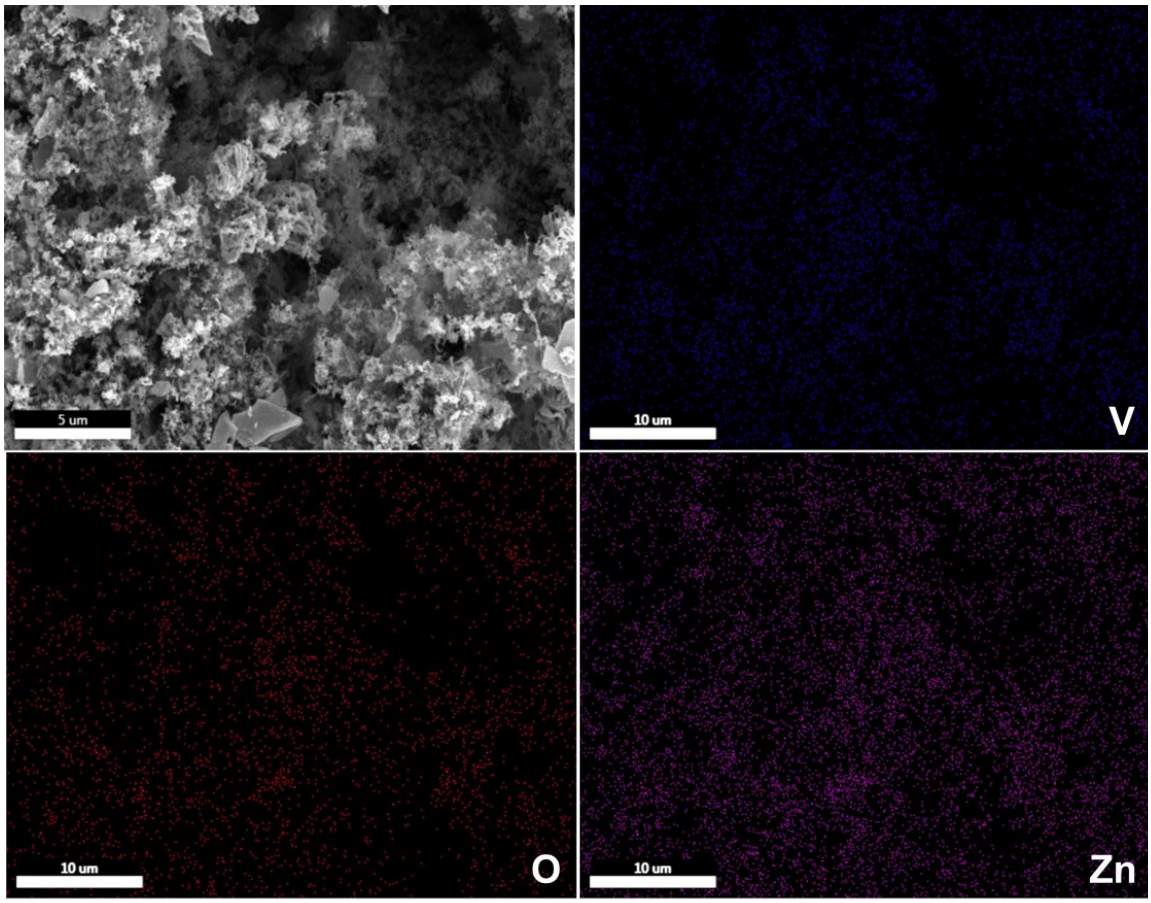

Figure S23. EDS mapping of $Mg_{0.23}V_2O_5 \cdot 1.0H_2O$ microspheres after fully discharge.

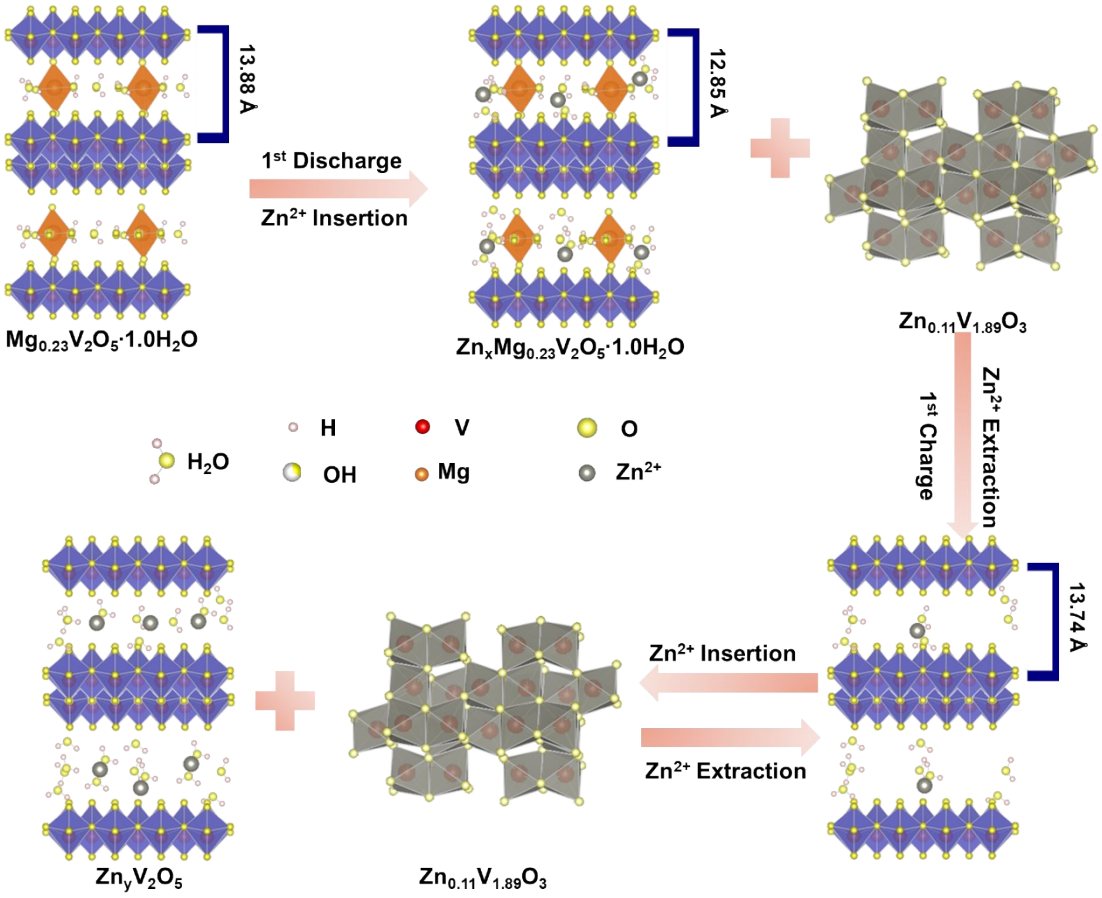

Figure S24. Schematic illustrations of Zn^{2+} storage during charge discharge process.

Table S1. Summary of electrochemical performance of cathode materials for solid-state ZIBs.

Cathode	Operating voltage	Current rate	Capacity[mAh/g]	Cycle performance	Ref.
Our MVO/Zn solid-state batteries	**0.2-1.6 V**	**5 A/g** **20 A/g**	**216 mAh/g** **82.3 mAh/g**	**98.6% retention after 2000 cycles** **70 % retention after 12000 cycles**	
VS_2	0.4-1.0 V	0.2 A/g	120 mAh/g	250 cycles	[22][1]
$NH_4V_3O_8$	0.2-1.4 V	0.5 A/g	133 mAh/g	200 cycles	[23][2]
MnO_2 nanocrystallites	0.8-1.9 V	0.131 A/g	135.2 mAh/g	1000 cycles	[24][3]
zinc orthovanadate	0.4-1.5 V	4 A/g	125 mAh/g	2000 cycles	[25][4]
MnO_2	1.0-2.0 V	1.3 A/g	127 mAh/g	1000 cycles	[26][5]
α-MnO_2	0.9-2.0 V	2.772 A/g	100 mAh/g	1000 cycles	[27][6]
MnO_2/PEDOT	0.9-1.8 V	1.11 A/g	280 mAh/g	300 cycles	[28][7]
$NaV_3O_8{\cdot}1.5H_2O$	0.3-1.25 V	0.5 A/g	~125 mAh/g	120 cycles	[29][8]
MnO_2	0.9-1.9 V	1.232 A/g	190 mAh/g	1000 cycles	[30][9]
VS_2	0.4-1.0 V	0.5 A/g	128 mAh/g	200 cycles, 91% of initial capacity	[31][10]
MoS_2	0.3-1.5 V	1 A/g	~150 mAh/g	500 cycles, 97.7% of initial capacity	[32][11]
MnO_2	0.9-1.9 V	0.924 A/g	~150 mAh/g	100 cycles	[33][12]
MnO_2	0.9-1.8 V	2.4 A/g	146 mAh/g	600 cycles, 87% of initial capacity	[34][13]
FeHCF	0-2.3 V	3 A/g	57 mAh/g	100 cycles	[35][14]
$Co_{0.247}V_2O_5{\cdot}0.944H_2O$	0.6-2.2 V	4 A/g	200 mAh/g	5500 cycles, 94.5% of initial cycle	[36][15]

NiCo	1.2-2.0 V	96 C	70 mAh/g	16000 cycles, 65% of initial cycle	[37][16]
$CoFe(CN)_6$	0.75-2.0 V	2 A/g	110 mAh/g	2000 cycles	[38][17]
δ -MnO_2	0.9-1.9 V	10 C	~100 mAh/g	55 cycles	[39][18]

Reference

1 Wang, Z. *et al.* A MOF-based single-ion Zn2+ solid electrolyte leading to dendrite-free rechargeable Zn batteries. *Nano Energy* **56**, 92-99 (2019).

2 Lai, J., Tang, H., Zhu, X. & Wang, Y. A hydrated NH 4 V 3 O 8 nanobelt electrode for superior aqueous and quasi-solid-state zinc ion batteries. *Journal of Materials Chemistry A* **7**, 23140-23148 (2019).

3 Wang, Z. *et al.* A flexible rechargeable zinc-ion wire-shaped battery with shape memory function. *Journal of Materials Chemistry A* **6**, 8549-8557 (2018).

4 Chao, D. *et al.* A high-rate and stable quasi-solid-state zinc-ion battery with novel 2D layered zinc orthovanadate array. *Advanced Materials* **30**, 1803181 (2018).

5 Zhang, S. *et al.* An adaptive and stable bio-electrolyte for rechargeable Zn-ion batteries. *Journal of Materials Chemistry A* **6**, 12237-12243 (2018).

6 Li, H. *et al.* An extremely safe and wearable solid-state zinc ion battery based on a hierarchical structured polymer electrolyte. *Energy & Environmental Science* **11**, 941-951 (2018).

7 Zeng, Y. *et al.* Achieving Ultrahigh Energy Density and Long Durability in a Flexible Rechargeable Quasi-Solid-State Zn–MnO2 Battery. *Advanced Materials* **29**, 1700274 (2017).

8 Wan, F. *et al.* Aqueous rechargeable zinc/sodium vanadate batteries with enhanced performance from simultaneous insertion of dual carriers. *Nature communications* **9**, 1-11 (2018).

9 Wang, D. *et al.* A Nanofibrillated Cellulose/Polyacrylamide Electrolyte-Based Flexible and Sewable High-Performance Zn–MnO2 Battery with Superior Shear Resistance. *Small* **14**, 1803978 (2018).

10 Jiao, T. *et al.* Binder-free hierarchical VS 2 electrodes for high-performance aqueous Zn ion batteries towards commercial level mass loading. *Journal of Materials Chemistry A* **7**, 16330-16338 (2019).

11 Li, H. *et al.* MoS2 nanosheets with expanded interlayer spacing for rechargeable aqueous Zn-ion batteries. *Energy Storage Materials* **19**, 94-101 (2019).

12 Liu, Z. *et al.* A mechanically durable and device-level tough Zn-MnO2 battery with high flexibility. *Energy Storage Materials* **23**, 636-645 (2019).

13 Mo, F. *et al.* A flexible rechargeable aqueous zinc manganese-dioxide battery working at–20° C. *Energy & Environmental Science* **12**, 706-715 (2019).

14 Yang, Q. *et al.* Activating C-Coordinated Iron of Iron Hexacyanoferrate for Zn Hybrid-Ion Batteries with 10 000-Cycle Lifespan and Superior Rate Capability. *Advanced Materials* **31**, 1901521 (2019).

15 Ma, L. *et al.* Achieving Both High Voltage and High Capacity in Aqueous Zinc-Ion Battery for Record High Energy Density. *Advanced Functional Materials* **29**, 1906142 (2019).

16 Huang, Y. *et al.* Solid-State Rechargeable Zn//NiCo and Zn–Air Batteries with Ultralong Lifetime and High Capacity: The Role of a Sodium Polyacrylate Hydrogel Electrolyte. *Advanced Energy Materials* **8**, 1802288 (2018).
17 Ma, L. *et al.* Achieving High-Voltage and High-Capacity Aqueous Rechargeable Zinc Ion Battery by Incorporating Two-Species Redox Reaction. *Advanced Energy Materials* **9**, 1902446 (2019).
18 Wang, D. *et al.* A Superior δ-MnO2 Cathode and a Self-Healing Zn-δ-MnO2 Battery. *ACS nano* **13**, 10643-10652 (2019).